JOURNAL OF MATERIALS SCIENCE 27 (1992) 3215–3220

Identification of the metastable phase α'_m in a Zn/Al alloy containing Cu and Mg

M. DURMAN
Istanbul Technical University, Sakarya Engineering Faculty, Department of Metallurgy, 54188 Adapazari, Turkey

S. MURPHY
Aston University, The Aston Triangle, Birmingham B4 7ET, UK

Samples of the commercial pressure-diecast alloy ZA8 containing 8.1% Al, 1.1% Cu and 0.024% Mg have been examined by transmission electron microscopy (TEM). During decomposition of the high temperature fcc β phase, on cooling after casting, a transitional phase was formed within the α phase in both dendrites and eutectic. This phase was identified as the metastable phase α'_m containing 11% Al or 23% Al, with a fcc crystal structure and lattice parameter (at 11%) of about 0.394 nm. It had adopted a symmetrical cube/cube orientation relationship with the surrounding fcc α phase. The stability of this metastable phase at ambient temperatures was greatly increased by the presence of copper.

1. Introduction

Despite the extensive use of zinc-rich alloys as commercial pressure-diecasting materials, little is known about the effects of the various alloying additions on their microstructure and hence on their properties. This is particularly important since the phase relationships in the ternary system Al/Cu/Zn on which they are based are complex [1–4], transitional phases are formed in fast-cooled material [5–9], and the relatively low melting points of the phases present, allow extensive mobility of the atomic species at near ambient temperatures so that phase changes can occur in service [10, 11].

A lot of basic experimental work has been done on binary Al/Zn alloys to determine the sequences of solid-state transformations by which the zinc-rich high temperature phases are converted to the equilibrium phases. The products depend on composition, cooling rate and ageing temperature [8, 9, 12, 13].

In alloys with approximately monotectoid composition it has been established that the high temperature fcc α′-phase is transformed into the low temperature, equilibrium phases α + η by two modes of transformation. One is a continuous decomposition of the supersaturated solid solution through the formation of spinodal zones followed by nucleation and growth of a sequence of intermediate, transitional phases with increasing zinc content or size

$$\alpha' \rightarrow \alpha + \alpha''_m \rightarrow \alpha + \alpha'_t + \alpha'_m \rightarrow \alpha + \eta$$

where α is the stable, aluminium-rich fcc phase with approximately 10% Zn, η is cph zinc with about 0.5% Al, α''_m is a coherent, zinc-rich precipitate with a rhombohedral modification of its fcc structure cell brought about by coherency stresses, and α'_m is an intermediate fcc phase with a high zinc content. Toldin *et al.* [12, 13] found that α'_t, the intermediate fcc aluminium-rich solid solution in equilibrium with α'_m was itself a metastable phase containing excess zinc which could decompose on ageing to form α + η.

The other transformation sequence involves a cellular reaction initiated at the α′ grain boundaries in which the products are $\alpha'_t + \alpha'_m$, both of which are converted to α + η on further ageing.

In the higher-zinc eutectoid alloys the phase transformations occur much more rapidly, but are similar, except that the η phase forms together with the α'_m directly from the β phase (which is structurally similar to the α′, but with higher zinc content), instead of via the α'_m phase.

Alloying additions can have a great influence on decomposition reactions. Magnesium slows down the transformations and suppresses the formation of η in the cellular reaction. At low ageing temperatures η is still formed by the cellular reaction and $\alpha'_t + \alpha'_m$ by the continuous reaction, but at higher temperatures even in eutectoid alloys the first products of the cellular reaction are $\alpha'_t + \alpha'_m$ and in monotectoid alloys the transitional phases α''_m and α'_m [13]. Copper delays decomposition reactions, and introduces a transitional ε-phase if the solid solubility of copper in the matrix is exceeded, but transitional phases similar to those in the binary Zn–Al system have been detected by X-ray diffraction (XRD) studies on quench-ageing [14, 15].

In all these alloys, much of the evidence for the phase transformations has been obtained from X-ray studies, which identify the phases present, but provide little information on the morphologies or association of the phases with each other, or on the mechanisms of

0022–2461

their formation and removal. Detailed electron microscopical studies are rare, and unambiguous identification of the transitional phases has not been accomplished. In particular, the structures of alloys in the near-eutectic composition range occupied by the most widely used commercial zinc diecasting alloys have been virtually ignored. In the as-cast state in which commercial alloys are used, these problems are compounded by a high degree of structural heterogeneity consequent upon the formation of primary and eutectic solidification structures and the effects of rapid cooling during and after solidification.

In this work transmission electron metallography was used to carry out an examination of the fine-scale metallurgical structure of a commercial zinc-rich diecasting alloy ZA8. This is an hypereutectic alloy (8% Al) which solidifies as primary β in a ($\beta + \eta$) eutectic matrix. The alloy was aged at ambient temperature for over five years after cold-chamber pressure diecasting, to achieve structures typical of castings about half-way through their possible service life. The object of the study was to determine whether the transitional phases found in experimental alloys played any significant role in material subject to the rapid solidification, cooling and ageing regime experienced by commercial diecastings, and the extent of any changes brought about by long-term ageing at ambient temperatures.

2. Experimental procedure

Zinc alloy pressure-diecastings made from commercial ZA8 ingot stock and aged for a period in excess of five years were supplied by Pasminco Europe for this study. Analysis by atomic absorption spectroscopy (AAS) gave the following composition

Zn–8.1% Al; 1.06% Cu; 0.024% Mg; $< 0.01\%$ Fe

These were typically thin-walled castings approximately 250 mm long by 50 mm wide by 2.18 mm thick, with additional shallow ribs and bosses, and the metallography was carried out on samples cut from the thinner parts of the casting.

TEM work was carried out on thin foil samples prepared using a conventional disc-jet method and a perchloric acid/ethanol based electrolyte. Final thinning of the discs was carried out by electropolishing in a double-jet Tenupol electropolisher. Good results were obtained using a current density of 0.28–0.37 A cm^{-2} at a temperature in the range -15 to $-25\,^{\circ}C$.

The thin foils were examined using a Philips EM400T instrument equipped with a scanning transmission electron microscopy (STEM) attachment and a quantitative energy dispersive spectroscopy (EDS) analytical system, at 100 keV. Conventional TEM was used to produce high-resolution images, selected area diffraction patterns (SADP) and convergent beam diffraction patterns (CBDP). The STEM mode of operation was used to obtain a highly-focussed beam of small diameter in order to determine the average chemical compositions of small phases from their characteristic X-ray emission. Analyses were carried out on thin parts of the foils to minimize errors due to particle/matrix overlap. A special beryllium sample holder was used for analytical work to cut down spectral interferences from that source.

For chemical analysis by EDS, the intensities of the characteristic X-ray peaks from the elements of interest were obtained by counting for live times of between 200 and 500 s, using interpolated background subtraction, and quantitative analyses were computed from the peak intensities using atomic number corrections only.

3. Results

3.1. Eutectic structures in ZA8

Fig. 1 is a conventional TEM bright-field (BF) low-magnification micrograph of the casting, showing a number of small, decomposed former β primary dendrites about 3–5 μm in diameter, set in a lamellar eutectic. A few pseudoprimary η particles, normally found in hypoeutectic alloys, were also present due to solidification under the extremely high cooling rates achieved in pressure-diecasting. The eutectic had solidified initially as a matrix of η phase with embedded β plates, and the numerous grain boundaries visible in this micrograph show that it was subdivided into small grains about 5–10 μm in size. During cooling to ambient temperature, the eutectic β phase had decomposed to form numerous small plates or rows of particles embedded in the η matrix. When viewed at higher magnification, Fig. 2, it was apparent that in the middle of many of these plates or particles were smaller, rounded or elongated particles some 35–200 nm in diameter, often exhibiting darker contrast than the surrounding material, and with distinct boundaries.

Quantitative chemical analysis using EDS was carried out on the three phases marked on Fig. 2, the η matrix (1), the outer part of the particulate phase (2) and the internal particle (3). At least ten analyses were carried out on different examples of each phase, and

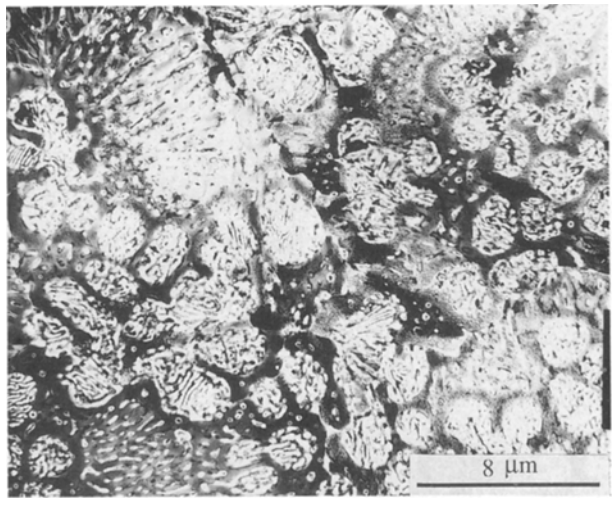

Figure 1 Conventional TEM BF micrograph showing numerous small, rounded primary β dendrites, and an interdendritic eutectic made up of polycrystalline η with small grains of α containing embedded particles or plates of α'_m.

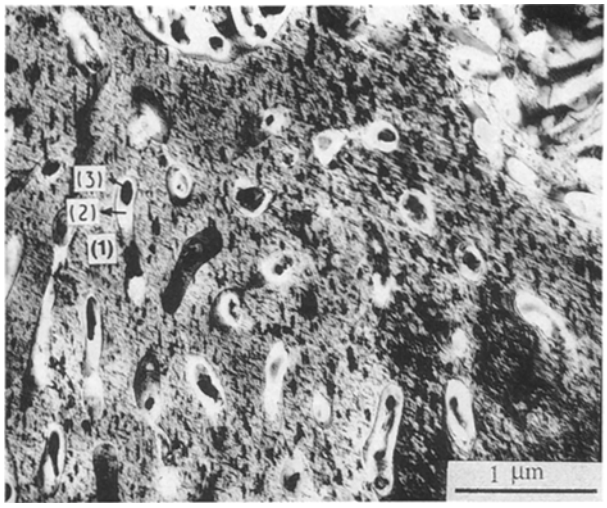

Figure 2 High magnification BF micrograph of eutectic region, showing irregular ribbon-like lamellae of α phase in polycrystalline η matrix. Most of the α contains second phase particles of α'_m. Numbers indicate phases chemically analysed by EDS.

the results are shown in Table I. In these analyses the aluminium:zinc ratio is considered to be correct, but the magnesium contents are undoubtedly much too high, and other work has indicated that the copper contents may be slightly overestimated too. These effects are probably due to an anomalous surface film formed on the thin foils during electropolishing. Taking these reservations into account, the results shown in Table I indicated that the matrix was zinc (η) with a higher than average copper content, the outer part of the particulate phase was an α-aluminium solid solution containing a substantial zinc content, and the third phase was a zinc-rich phase containing 11% Al. Both of the latter two phases also contained some copper. The α and η phases are near-equilibrium phases, but the zinc-rich internal precipitate did not correspond to any phase of the Zn/Al/Cu system which is stable at ambient temperatures.

Convergent beam diffraction was used to obtain electron diffraction patterns from the unknown phase, and an example is shown in Fig. 3. This diffraction pattern was from a $\langle 1\,1\,0\rangle_{fcc}$ zone. A diffraction pattern was also obtained from the α-phase matrix beside the metastable phase, which gave an identical zone with the reflections parallel to the corresponding ones in the transitional phase, indicating that the two crystal lattices were exactly parallel, i.e. that the two crystals had the cube/cube orientation relationship. From the known zinc content of 22% in the matrix α, its lattice parameter was estimated as $a = 0.4028$ nm, and this was used as a calibration to determine the lattice parameter of the unknown fcc phase as $a = 0.394$ nm. The fcc structure cell, aluminium content of 11% and small lattice parameter identify it as the zinc-rich transitional α'_m phase found in binary zinc/aluminium alloys on quench-ageing [5–7].

Examination of Figs 1 and 2 showed that the η matrix contained heterogeneously-nucleated precipitates forming a very high density dispersion throughout the matrix. The high over-all copper content of the

TABLE I Mean EDS compositions of the phases in ZA8 alloy (wt%)

Phase		Zn	Al	Cu	Mg
η matrix;	Fig. 2 (1)	95.8	0.5	3.4	0.4
α-phase;	Fig. 2 (2)	22.1	75.2	2.0	0.7
α'_m;	Fig. 2 (3)	86.8	11.0	1.9	0.3
η matrix;	Fig. 6 (4)	95.0	1.1	3.3	0.4
α-phase;	Fig. 6 (5)	16.2	82.3	0.8	0.6
α'_m;	Fig. 6 (6)	75.7	22.8	1.4	0.1

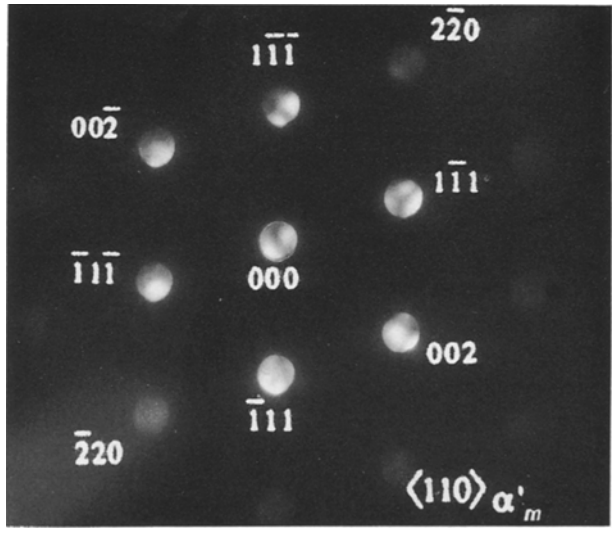

Figure 3 CBDP showing $\langle 1\,1\,0\rangle_{fcc}$ zone from transitional phase particle with lattice parameter $a = 0.394$ nm.

η regions revealed by EDS analyses together with the known low solubility of copper in η at ambient temperatures [16], suggested that these precipitates were a copper-rich phase formed on cooling after casting, and the phase was identified from electron diffraction patterns as the ε-phase $CuZn_4$ with $a = 0.274$ nm, $c = 0.429$ nm, $c/a = 1.567$. This is reported in detail elsewhere [17].

3.2. β-phase decomposition structures

Solid-state transformation of the primary β-phase dendrites into final products with different morphologies on cooling below the eutectoid temperature is shown in the BF micrographs of Fig. 4, which shows the particulate products, and Fig. 5 which shows the lamellar forms developed in the interior parts of the prior β dendrites. In both of these micrographs the η-phase contained ε-phase precipitates and the α-phase was free from general precipitates but contained small rounded particles similar to those identified as α'_m in the eutectic. In Fig. 4, the generally convex shapes of the η-phase particles indicated that these had grown into the fcc matrix, and their numerous interconnections suggested that they were only partially particulate, and had formed as complex, interwoven tubular structures about 200 nm in width, similar to those in the decomposed eutectic. The lamellar products of Fig. 5 appeared to have developed from the jumble of intermixed phases at the edge of a dendrite, and

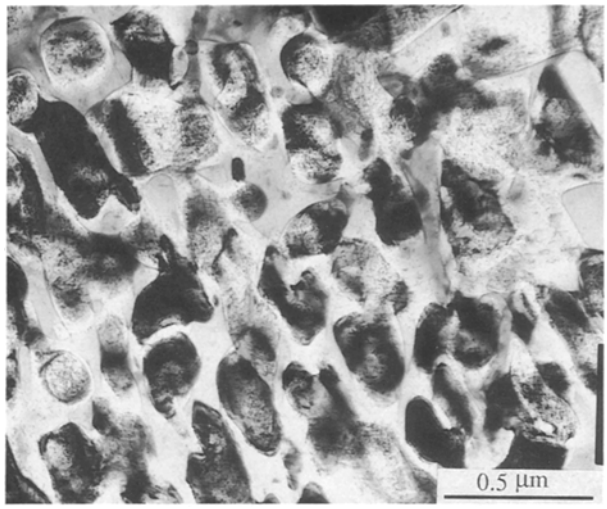

Figure 4 BF micrograph of decomposed primary β, showing complex intergrowth of α and η phases, with small amount of α'_m.

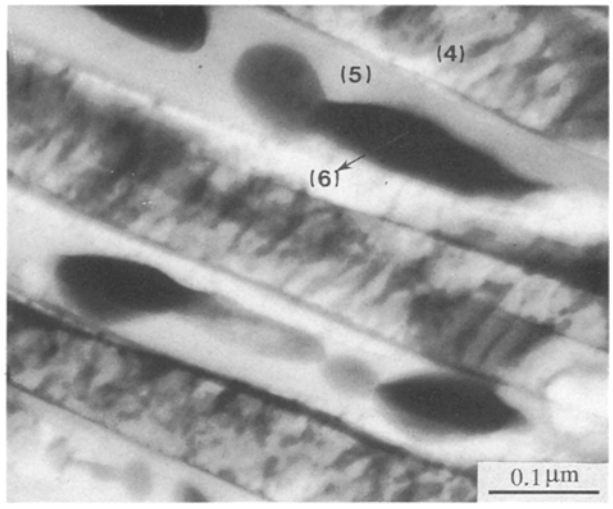

Figure 6 Higher magnification BF micrograph of same area as Fig. 5, numbers identify phases analysed by EDS.

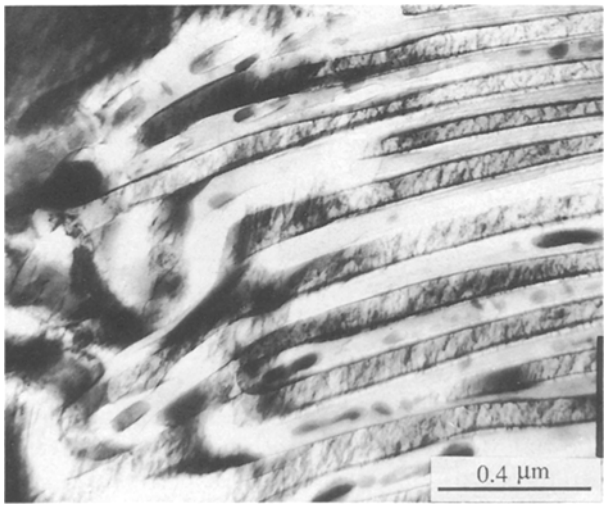

Figure 5 BF micrograph of former β dendrite now decomposed into lamellar α and η with centrally disposed α'_m in the α phase lamellae.

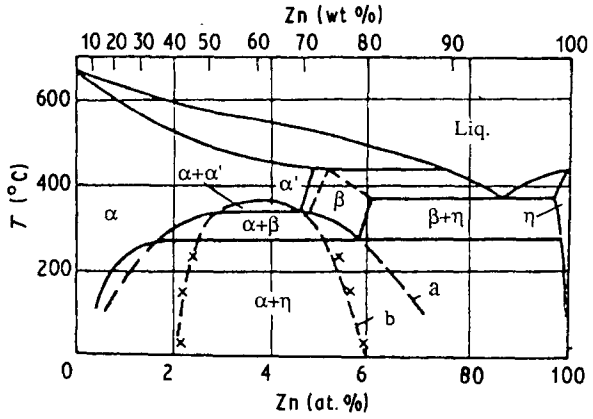

Figure 7 Diagram of the Al/Zn system after Toldin *et al.* [13] showing the positions of the metastable phase boundaries.

rapidly achieved a regular lamellar morphology of α and η plates with a spacing of about 150 nm. The η and α lamellae were about equal in thickness.

Fig. 6 is a higher magnification BF micrograph of the lamellar products, showing the strings of metastable particles within the α matrix. Using the STEM mode to produce a highly-focussed beam, the various phases marked in Fig. 6 were quantitatively analysed. At least five analyses were carried out on each phase, and the mean results are shown in Table I. The η and α phases were of approximately the same composition as those in the eutectic, but the transitional phase had a higher aluminium content (22.8%) and a lower copper content. Apart from this difference in transitional phase composition, it appeared that the phases produced by the decomposition of the primary dendrites in ZA8 were similar to those formed by decomposition of the eutectic.

4. Discussion

4.1. Decomposition of the β-phase

The decomposition of the β-phase which forms part of the eutectic phase mixture in many zinc-based alloys has been shown to result in the formation of a transitional phase with high zinc content and fcc crystal structure. Such phases have been found in quench-aged, zinc-based alloys with much higher aluminium contents, and they are thought to result from the spinodal decomposition of the high temperature α'-phase of the Zn/Al system [5–9, 12, 13], and from certain discontinuous reactions in which unstable β is converted to more stable products [9, 12, 13].

In the Al/Zn phase diagram, a metastable miscibility gap has been proposed [13], which indicates the compositions of the products of such a reaction, and this is shown, with the phase fields relabelled according to our convention, in Fig. 7. Extrapolation of the β solubility curve to near ambient temperature indicates that the expected composition of the high-zinc phase would lie very close to the measured composition of the transitional phase found here in the eutectic. Thus it is possible that an eutectic β-phase with an aluminium content of approximately 19% could form transitional phases α'_t and α'_m with fcc structures and aluminium contents of about 75 and 11%, respectively.

The results obtained in this study suggest a possible mechanism for the decomposition of the unstable

β-phase in contact with eutectic η, which explains the experimental observation of a central distribution of zinc-rich, transitional phases within the former β plates. If on cooling through the eutectoid temperature, high-aluminium fcc α-phase was nucleated on both η/β interfaces of an fcc β plate in the lamellar eutectic and grew inwards into the β, partitioning of aluminium and zinc across the new surfaces would occur. The α in contact with the zinc matrix would be expected to rapidly achieve the equilibrium composition, but in view of the known metastable miscibility gap in the Al–Zn system, a metastable equilibrium would be set-up across the inner surface so that the β on one side adopted the composition of α'_m, and the α on the other side adopted the higher-zinc composition of α'_t. The zinc concentration of 22% measured in the aluminium-rich phases probably represents some intermediate value between the stable and transitional extremes of composition. Inward growth of the high-aluminium surface layers would proceed rapidly, aided by the diffusion of aluminium atoms down the concentration gradient between β and α'_m until all the β was replaced by α'_m. At that point in the transformation, although the aluminium content of the central region would have been nearly halved from 19 to 11%, the surface layers would still be comparatively narrow due to their high aluminium content (75–85%). Continued growth of the α must then proceed at a reducing rate due to the increasing diffusion distance for the zinc atoms from the α'_m through the α layer to the η phase, but the long-term persistence of the metastable phase indicates that the bulk free energy of α'_m did not differ much from that of η, and that the surface energy of the α'_m/α'_t boundary was small. The similar crystal structures and cube/cube orientation relationship observed here support the latter conclusion, but the observation that the central α'_m layer had broken up into strings of rounded particles on ageing to minimize the surface area suggests that the small bulk free energy difference was the more important factor. Copper appears to have had a strong effect in stabilizing the α'_m, since a recent study of the commercial alloy No. 3 (BS 1004 Alloy A) which had a similar but copper-free eutectic, was found to contain similar α'_m particles shortly after casting, but virtually none after ageing for the same period of time as the ZA8 alloy studied in this work [18].

The higher aluminium content of the α'_m in the decomposition products of the former β dendrites may be linked to a higher aluminium content of the original β-phase which would be expected at least in their interior regions, due to their formation above the eutectic temperature. The mechanism of formation of the lamellar products of the solid-state transformation is not known, but if the residual α'_m was derived in some way from a higher-aluminium β than that of the eutectic, a bigger change would be needed to reach the metastable composition of near 11% Al. The much larger scatter in the analysed aluminium contents of the transitional phases shown in Table I may thus be a result of genuine variations between different particles. Alternatively, higher-aluminium metastable phases have been identified in a previous study [13] whose compositions are given by extrapolation of the α/α' boundary of the monotectoid two-phase field of Fig. 7 to near-ambient temperatures. This would indicate a composition near to the measured value of 23% Al, suggesting that the transitional phase in the decomposed dendrites might be better described as a metastable form of β rather than α'_m.

4.2. Effects of copper and magnesium on properties

It is significant that both the copper-containing ε-phase and α'_m were found in considerable amounts in an alloy which had been aged at ambient temperatures for over five years, although neither are stable in alloys of this composition at ambient temperatures. The absence of transitional α'_m phase in the eutectic in the alloy No. 3 [18] with similar magnesium content to ZA8, but containing no copper, after a similar ageing period to ZA8 suggests that copper must stabilize the α'_m phase, whereas magnesium had a small or no effect. Copper has been shown to improve the mechanical properties of zinc–aluminium alloys, and the highly-persistent, fine dispersion of metastable ε-phase precipitates in the dominant η phase of ZA8 is undoubtedly the reason for that effect.

Magnesium even at the low level used in this alloy is also known to improve the mechanical properties, but the effects of this element on the microstructure were not directly apparent. Magnesium was apparently not concentrated preferentially in any of the phases and no magnesium-rich compounds were detected, so its role remains unclear.

5. Conclusions

1. The cast alloy had solidified to form small, primary β dendrites of ~ 3–5 μm in diameter, together with some *pseudo*primary η particles, set in an eutectic matrix of β + η. These structures are consistent with solidification under conditions of high undercooling.
2. The high-temperature β-phase of the primary dendrites had subsequently decomposed on cooling below the eutectoid temperature to form semi-particulate, intergrown structures at the edges, and well-formed lamellar products with an interlamellar spacing of about 150 nm in the interiors.
3. Two of the β-decomposition products in both the dendrites and the eutectic were identified as α and η phases with average compositions which corresponded closely to the equilibrium compositions at ambient temperatures, except that copper was preferentially segregated into the η-phase. A third phase located at the centres of the α-phase particles or plates was identified as a metastable phase, α'_m, found in quench-aged zinc–aluminium alloys with much higher aluminium contents.
4. The α'_m phase in the eutectic α contained 11% Al and in the dendritic α 23% Al, and had an fcc structure with a lattice parameter estimated as $a = 0.394$ nm, 2% smaller than that of the α-phase matrix in which it was enclosed. It had adopted a

symmetrical cube/cube orientation relationship with that phase.

5. The mechanism of formation of α'_m from eutectic β is not known, but the location of the transitional phase in the middle of the resulting α-phase suggests a mechanism for the decomposition of the original β-phase involving the nucleation of α against the η-phase and its inward growth into the β, the α and β phases across the inner interface adopting the compositions of transitional phases in metastable equilibrium. The role of α'_m in the decomposition of dendritic β is not known, but an analogous mechanism of formation may apply.

6. Copper was found to delay the eventual dissolution of α'_m and its replacement by the $\alpha + \eta$ phases, an effect attributed to a reduction of its bulk free energy to a level close to that of the stable η-phase.

Acknowledgements

This work was carried out in the Department of Mechanical and Production Engineering at Aston University, to whom thanks are due for the provision of facilities. The majority of the TEM work was carried out using the instruments at the University of Birmingham whose help in the provision of high-resolution TEM facilities is gratefully acknowledged. The authors are also grateful for the financial support of the Republic of Turkey for one of the authors and the unstinting assistance and generous support of Pasminco (Europe) Ltd in furthering this work.

References

1. W. KOSTER and K. MOELLER, *Z. Metallkunde* **33** (1941) 278.
2. E. GEBHARDT, *ibid.* **34** (1942) 208.
3. H. H. ARNDT and K. MOELLER, *ibid.* **51** (1960) 596.
4. S. MURPHY, *ibid.* **71** (1980) 96.
5. R. D. GARWOOD, A. L. DAVIES and G. L. RICHARDS, *J. Inst. Met.* **88** (1959–60) 375.
6. M. SIMERSKA and V. SYNECEK, *Acta Metall.* **15** (1967) 223.
7. G. J. C. CARPENTER and R. D. GARWOOD, *Met. Sci. J.* **1** (1967) 202.
8. A. KRUPKOWSKI, R. CIACH and J. KROL, *Bull. Acad. Pol. Sci.* **15** (1967) 975.
9. V. A. TOLDIN, G. V. KLESHCHEV, D. V. SHUMILOV and A. J. SHEYNKMAN, *Fiz. Metal. Metalloved.* **40** (1975) 1223.
10. S. MURPHY, N. MYKURA and Y. H. ZHU, *Canad. Met. Quart.*, **25** (1986) 145.
11. N. MYKURA, S. MURPHY and Y. H. ZHU, *Mat. Res. Soc. Proc.* **21** (1984) 841.
12. V. A. TOLDIN, A. A. BURYKIN and G. V. KLESHCHEV, *Phys. Met. Metall.* **45** (1978) 97.
13. *Idem, ibid.* **51** (1981) 116.
14. R. CIACH, J. KROL and K. WEGRZYN-TASIOR, *Bull. Acad. Pol. Sci.* **17** (1969) 371.
15. G. WENDROCK, B. MAJOR, H. LÖFFLER, K. GRABIANOWSKA and R. CIACH, *Crys. Res. Tech.* **16** (1981) 837.
16. M. HANSEN and K. ANDERKO, in "Constitution of Binary Alloys" 2nd Edn (McGraw-Hill, 1958) p. 651.
17. M. DURMAN and S. MURPHY, *Acta Metall.*, **39** (1991) 2235.
18. M. DURMAN, K. SAWALHA and S. MURPHY, *Mat. Sci. Eng.* **A130** (1990) 247.

Received 18 February
and accepted 20 June 1991